

where  $E_{\parallel}$  and  $E_{\perp}$  are the  ${}^2B_1 \rightarrow {}^2B_2$  and  ${}^2B_1 \rightarrow {}^2E$  positive hole transitions, respectively;  $\zeta$  is the one-electron spin-orbit coupling parameter and  $\kappa$  is the orbital reduction factor.  $K_{\parallel}$  and  $K_{\perp}$  are the principal molecular susceptibilities parallel and perpendicular to the symmetry axis of the molecule.

As indicated above, there have been conflicting interpretations of the ordering and separation of the  ${}^2B_2$  (hole in  $d_{xy}$ ) and  ${}^2E$  (hole in  $d_{xz}$ ,  $d_{yz}$ ) states, as inferred from the electron spin resonance studies. For instance, the relative ordering of these two states as deduced recently by Harrison and Assour<sup>12</sup> ( ${}^2B_2$  being above the  ${}^2E$ ) is at variance with the earlier calculation of Kivelson and Nieman<sup>10</sup> and also, to some extent, with that deduced by Gibson, *et al.*<sup>9</sup> However, Gibson, *et al.*, placed these two states very close together, and their calculation was somewhat uncertain because of their failure to observe the  ${}^{14}\text{N}$  superhyperfine structure which was observed by all later workers. Further, the magnitudes of  $E_{\parallel}$  and  $E_{\perp}$  deduced by various workers differ very widely among themselves. Roberts and Koski<sup>11</sup> have even taken the  $\pi$ - $\pi$  optical transitions of the organic ring as being the d-d transitions.

In Figure 1, we have plotted two theoretical curves with different  $E_{\parallel}$  and  $E_{\perp}$ , taking  $\zeta = 500 \text{ cm}^{-1}$  and  $\kappa^2 = 0.7$ . The solid curve has been drawn assuming  $E_{\parallel} = 27,000 \text{ cm}^{-1}$  and  $E_{\perp} = 17,000 \text{ cm}^{-1}$  which are very close to the values deduced by Harrison and Assour. The dashed curve has been drawn taking the values of  $E_{\parallel}$  and  $E_{\perp}$  deduced by Kivelson and Nieman (17,000 and 25,000  $\text{cm}^{-1}$ , respectively). The close agreement of our experimental results with the solid curve confirms the ordering of  ${}^2B_2$  and  ${}^2E$  states as deduced by Harrison and Assour (*i.e.*, as shown in Figure 2). The values of  $\zeta$  and  $\kappa$  assumed in the present calculation are in good agreement with the degree of covalency deduced from the observed  ${}^{14}\text{N}$  superhyperfine structure in this compound. For no reasonable values of  $\zeta$  and  $\kappa$  can our experimental data be fitted to the energy separations used by Kivelson and Nieman.

This result illustrates the usefulness of the para-

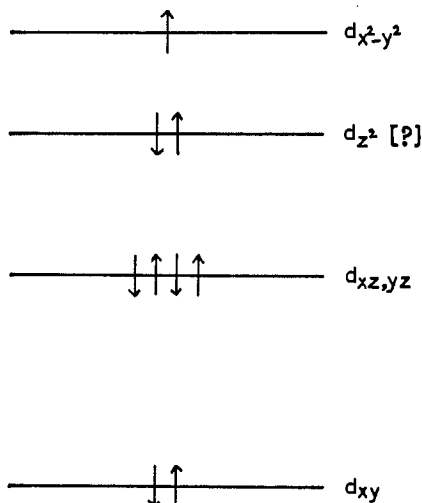


Figure 2.—A schematic representation of the electronic structure of  $\beta$ -copper(II) phthalocyanine.

magnetic anisotropy in deducing the electronic structure of square-planar copper compounds. Unfortunately, neither magnetic anisotropy nor electron spin resonance can be used to locate the relative position of the  ${}^2A_1$  state beyond confirming that it lies higher in energy than  ${}^2B_1$ .

**Acknowledgment.**—We thank Drs. P. E. Fielding and A. G. McKay for providing us with the single crystals of copper phthalocyanine.

CONTRIBUTION FROM THE CHEMISTRY DEPARTMENT,  
POLYTECHNIC INSTITUTE OF BROOKLYN,  
BROOKLYN, NEW YORK 11201

### Electronic Structure of $\text{CrO}_4^{3-}$ in $\text{Ca}_2(\text{CrO}_4, \text{PO}_4)\text{Cl}$

By C. SIMO,<sup>1</sup> E. BANKS, AND S. L. HOLT<sup>2</sup>

Received June 16, 1969

In the past 10 years there has been a rapidly increasing application of Wolfsberg-Helmholz type of molecular orbital calculations to the problem of electronic structure of transition metal ions.<sup>3-5</sup> It is interesting to note, however, that while this method is widely used, the original system to which this method was applied, namely,  $\text{MnO}_4^-$ , has yet to have its electronic structure satisfactorily described.<sup>6-10</sup> Indeed no small part of this problem has been the fact that until recently<sup>11</sup> all calculations pertaining to the  $\text{MnO}_4^-$  ion were based on inadequate data.

The study of  $\text{CrO}_4^{3-}$  was undertaken as part of a program to provide a sound experimental basis for calculations pertaining to the electronic structure of higher oxidation states.

Banks, Greenblatt, and McGarvey<sup>12</sup> reported the esr spectra of  $\text{CrO}_4^{3-}$ -doped single crystals of  $\text{Ca}_2\text{PO}_4\text{Cl}$  and showed that the unpaired electron is in an orbital having largely  $d_{z^2}$  character. They also reported some unpolarized absorption spectra at liquid nitrogen temperature showing bands at 37,250, 27,940, 24,500, and 17,400  $\text{cm}^{-1}$ . These were compared to the results of Carrington, *et al.*,<sup>13</sup> on  $\text{MnO}_4^{2-}$  and  $\text{CrO}_4^{3-}$  and were shown to be similar. Extended optical measurement, however, produced important new features<sup>14</sup> which

- (1) NSF-SDP postdoctoral fellow.
- (2) Author to whom correspondence should be addressed at the Chemistry Department, University of Wyoming, Laramie, Wyo. 82070.
- (3) H. Bedon, S. Horner, and S. Y. Tyree, *Inorg. Chem.*, **3**, 647 (1964).
- (4) F. A. Cotton and C. B. Harris, *ibid.*, **6**, 376 (1967).
- (5) H. Basch and H. B. Gray, *ibid.*, **6**, 639 (1967).
- (6) A. Viste and H. B. Gray, *ibid.*, **3**, 1113 (1964).
- (7) R. F. Fenske and C. C. Sweeney, *ibid.*, **3**, 1105 (1964).
- (8) L. Oleari, G. de Michelis, and L. de Sipio, *Mol. Phys.*, **10**, 111 (1966).
- (9) P. M. Schatz, A. J. McCaffery, W. Swetaka, G. N. Henning, A. B. Ritchie, and P. J. Stephens, *J. Chem. Phys.*, **45**, 722 (1966).
- (10) J. P. Dahl and H. Johansen, *Theoret. Chim. Acta*, **11**, 8, 26 (1968).
- (11) S. L. Holt and C. J. Ballhausen, *ibid.*, **7**, 313 (1967).
- (12) E. Banks, M. Greenblatt, and B. R. McGarvey, *J. Chem. Phys.*, **47**, 3772 (1967).
- (13) A. Carrington and D. S. Schonland, *Mol. Phys.*, **3**, 331 (1960).
- (14) E. Banks, M. Greenblatt, and S. Holt, *J. Chem. Phys.*, **49**, 1431 (1968).

we report in detail. We have also included a comparison of the results of molecular orbital approximations involving transition metal ions in high oxidation states with our experimental observations. A description and critical appraisal of these theories can be found in a recent comprehensive review.<sup>15</sup>

### Experimental Section

Solid phases with the spodosite structure, of composition  $\text{Ca}_2\text{XO}_4\text{Y}$ , where  $\text{X}^{5+} = \text{Cr}^{5+}$  or  $\text{P}^{5+}$  and  $\text{Y}^- = \text{OH}^-$ ,  $\text{Cl}^-$ , or  $\text{Br}^-$ , were first synthesized by Banks and Jaunarajs.<sup>16</sup> Single crystals of the chlorospodosites were grown from excess  $\text{CaCl}_2$  flux. Better crystals of  $\text{Ca}_2\text{PO}_4\text{Cl}$ ,  $\text{Ca}_2\text{CrO}_4\text{Cl}$ , and their solid solutions were grown in the same manner by Banks, Greenblatt, and Post,<sup>17</sup> who reported the crystal structures of the two end members of the solid solution series. The method of crystal growth was described in some detail by Kingsley, *et al.*,<sup>18</sup> who described and interpreted the absorption and fluorescence spectra of  $\text{MnO}_4^{3-}$ -doped  $\text{Ca}_2\text{PO}_4\text{Cl}$ .

$\text{Ca}_2\text{PO}_4\text{Cl}$  and  $\text{Ca}_2\text{CrO}_4\text{Cl}$  possess orthorhombic crystal symmetry with four  $\text{XO}_4^{3-}$  ions per unit cell.<sup>17</sup> Each X atom is at the center of a tetrahedron which is distorted in such a way as to have as its only symmetry element a twofold rotation axis perpendicular to the (100) crystal face. Angular distortions are such that the geometry of the molecule closely approximates  $D_{2d}$  symmetry, however.

Optical measurements and crystal face identification were made as reported in earlier publications from this laboratory.<sup>19-22</sup>

### Results

The complete polarized spectrum of  $\text{Ca}_2[\text{PO}_4\text{-CrO}_4]\text{Cl}$ , recorded at  $80^\circ\text{K}$ , is shown in Figure 1. Figure 2 shows the lowest energy band, recorded at liquid

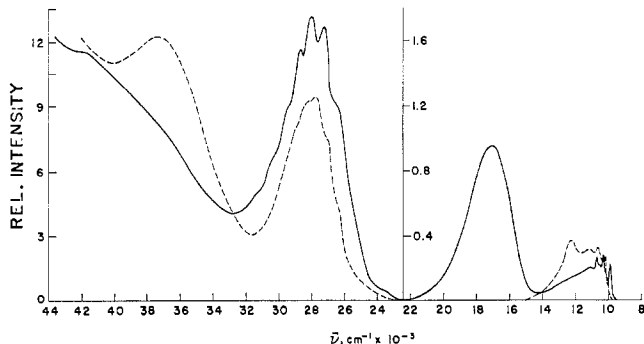


Figure 1.—The polarized spectrum of  $\text{CrO}_4^{3-}$  at  $80^\circ\text{K}$ .

helium temperature. The two most prominent features associated with this absorption manifold are the strongly polarized sharp lines on the low-energy end of the band and the less completely polarized manifold on the high-energy side of the band. These features are not apparent in the room-temperature spectrum but are exhibited in some detail at  $80^\circ\text{K}$ . The line spectra consist of four readily discernible components in the  $\parallel a$  ( $\parallel z$ ) polarization and five components in the

(15) J. P. Dahl and C. J. Ballhausen, *Advan. Quantum Chem.*, **4**, 170 (1968).

(16) E. Banks and K. L. Jaunarajs, *Inorg. Chem.*, **4**, 78 (1965).

(17) E. Banks, M. Greenblatt, and B. Post, *Acta Cryst.*, **23**, 166 (1967).

(18) J. D. Kingsley, J. S. Prener, and B. Segall, *Phys. Rev.*, **137A**, 189 (1965).

(19) S. L. Holt and A. Wold, *Inorg. Chem.*, **6**, 1594 (1967).

(20) C. Simo and S. Holt, *ibid.*, **7**, 2655 (1968).

(21) J. Milstein and S. L. Holt, *ibid.*, **8**, 1021 (1969).

(22) C. Simo, E. Banks, and S. L. Holt, *ibid.*, **8**, 1446 (1969).

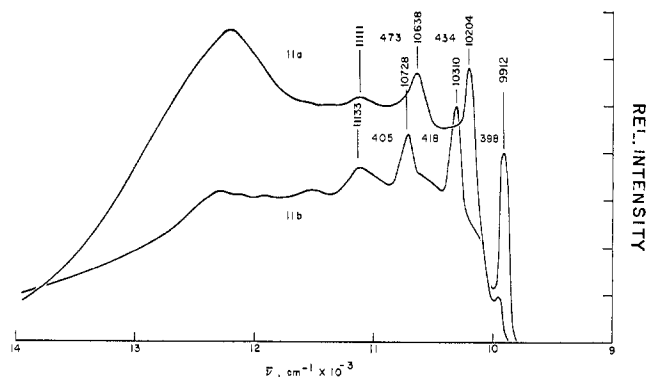


Figure 2.—The near-infrared spectrum of  $\text{CrO}_4^{3-}$  at  $5^\circ\text{K}$ . [The symbol  $\parallel a$  indicates that the electric vector of the incident radiation is parallel to the  $a$  crystallographic axis ( $\parallel z$  molecular axis);  $\parallel b = \perp z$ .]

$\parallel b$  ( $\perp z$ ) polarization. These lines are obviously associated with simultaneous electronic and vibrational excitations. Positions and spacing of these lines are given in Table I.

$\parallel a$		$\parallel b$	
$\bar{\nu}$ , $\text{cm}^{-1}$	$\Delta\bar{\nu}$ , $\text{cm}^{-1}$	$\bar{\nu}$ , $\text{cm}^{-1}$	$\Delta\bar{\nu}$ , $\text{cm}^{-1}$
		9,912	
			398
10,204		10,310	418
	434		
10,638		10,728	405
	473		
11,111		11,133	

The 15,000-21,000- $\text{cm}^{-1}$  manifold is devoid of fine structure. Indeed, it consists of a completely polarized broad band centered at  $\sim 17,100 \text{ cm}^{-1}$  with a weak shoulder on the low-energy side at  $\sim 15,400 \text{ cm}^{-1}$ .

Figure 3 displays the 24,000-31,000- $\text{cm}^{-1}$  region of

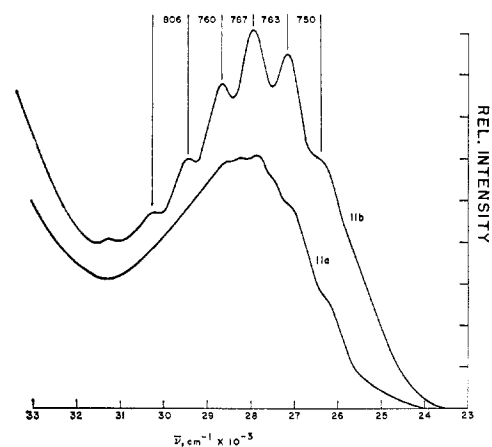


Figure 3.—The visible spectrum of  $\text{CrO}_4^{3-}$  at  $5^\circ\text{K}$ .

the absorption. The well-defined vibrational structure exhibited by the  $\parallel b$  polarization is tabulated in Table II.

TABLE II  
VIBRATIONAL COMPONENTS IN THE 24,000–31,000-CM<sup>-1</sup>  
REGION OF THE SPECTRUM OF Ca<sub>2</sub>[PO<sub>4</sub>CrO<sub>4</sub>]Cl

$\bar{\nu}$ , cm <sup>-1</sup>	$\Delta\bar{\nu}$ , cm <sup>-1</sup>	$\bar{\nu}$ , cm <sup>-1</sup>	$\Delta\bar{\nu}$ , cm <sup>-1</sup>
26,420		28,690	
	750		760
27,170		29,450	
	763		806
27,933		30,256	
	767		

### Discussion

**Band Assignment.**—Of the four major absorption bands which occur between 8000 and 44,000 cm<sup>-1</sup>, three can be unequivocally assigned in D<sub>2d</sub> symmetry (Table III, Figure 4). These assignments were arrived

TABLE III

Transition energy, cm <sup>-1</sup>	Allowed	Assignment in D <sub>2d</sub> symmetry
9,912	$\perp z$	${}^2A_1 \rightarrow {}^2E$
10,204	$\parallel z$	${}^2A_1 \rightarrow {}^2B_2$
17,000	$\perp z$	${}^2A_1 \rightarrow {}^2E$
26,420	$\perp z$	${}^2A_1 \rightarrow {}^2E$
26,000	$\parallel z$	${}^2A_1 \rightarrow {}^2E_2$

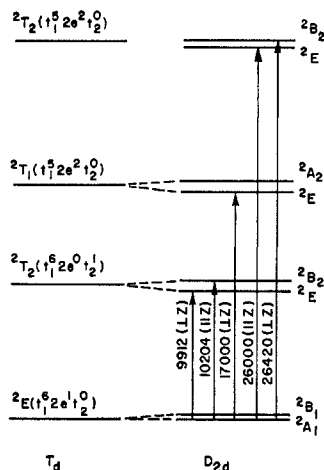


Figure 4.—The energy level diagram for CrO<sub>4</sub><sup>3-</sup>.

at in the following way. In the ground state the single unpaired electron has been shown to occupy a d<sub>2z</sub> orbital.<sup>12</sup> This orbital transforms as A<sub>1</sub> in D<sub>2d</sub> symmetry. Further, in D<sub>2d</sub> symmetry, transitions A<sub>1</sub> → E are allowed perpendicular to the z molecular axis while A<sub>1</sub> → B<sub>2</sub> transitions are allowed parallel to the z molecular axis. A<sub>1</sub> → A<sub>2</sub> excitations are forbidden in both polarizations. Most current molecular orbital treatments put the ordering of the one-electron levels of interest as t<sub>1</sub><sup>6</sup> < e<sup>1</sup> < t<sub>2</sub> (in T<sub>d</sub> symmetry). The lowest energy bands should thus arise from low-symmetry components of transitions associated with, in T<sub>d</sub> symmetry, the configuration t<sub>1</sub><sup>6</sup>e<sup>0</sup>t<sub>2</sub><sup>1</sup> or t<sub>1</sub><sup>5</sup>e<sup>2</sup>t<sub>2</sub><sup>0</sup>. The latter possibility can be ruled out in the following way. The configuration t<sub>1</sub><sup>5</sup>e<sup>2</sup>t<sub>2</sub><sup>0</sup> should give rise, in tetrahedral symmetry, to <sup>2</sup>T<sub>2</sub> and <sup>2</sup>T<sub>1</sub>, as well as quartet states while the configuration t<sub>1</sub><sup>5</sup>e<sup>0</sup>t<sub>2</sub><sup>1</sup> has only a <sup>2</sup>T<sub>2</sub> state associated with it. In D<sub>2d</sub> symmetry a <sup>2</sup>T<sub>2</sub> state splits into a <sup>2</sup>B<sub>2</sub>

and a <sup>2</sup>E while a <sup>2</sup>T<sub>1</sub> state gives rise to a <sup>2</sup>A<sub>2</sub> and a <sup>2</sup>E; cf. Figure 4. Based on the aforementioned selection rules and the fact that the low-symmetry splitting does not appear to be large (Figures 1 and 2), the band which occurs  $\perp z$  at  $\sim 17,000$  cm<sup>-1</sup> must be the allowed  ${}^2A_1 \rightarrow {}^2E$  component of the  ${}^2E \rightarrow {}^2T_1$  transition, while the manifolds at  $\sim 10,000$  and  $\sim 26,000$  cm<sup>-1</sup> must be associated with low-symmetry components of the  ${}^2E \rightarrow {}^2T_2$  transitions arising from the t<sub>1</sub><sup>6</sup>e<sup>1</sup>t<sub>2</sub><sup>0</sup> → t<sub>1</sub><sup>6</sup>e<sup>0</sup>t<sub>2</sub><sup>1</sup> and t<sub>1</sub><sup>6</sup>e<sup>2</sup>t<sub>2</sub><sup>0</sup> → t<sub>1</sub><sup>5</sup>e<sup>2</sup>t<sub>2</sub><sup>0</sup> excitations. [We exclude the possibility that the 10,000-cm<sup>-1</sup> manifold might arise from a spin doublet to spin quartet transition on the following bases: (1) the relative intensity, compared to that of the 17,000-cm<sup>-1</sup> band, is not low enough, (2) this would leave a spin-allowed transition unaccounted for, (3) no other spin-forbidden bands are observed although the t<sub>1</sub><sup>5</sup>e<sup>2</sup>t<sub>2</sub><sup>0</sup> configuration gives rise to more than one quartet state, (4) the intensities of the xy and the z components of a spin-forbidden transition would most likely be very different due to the  $\Delta E$  term of the equation  $f_{4,6} = f^0(a_{nl}^2/\Delta E)^2$ , which governs the oscillator strength of spin-forbidden transitions.<sup>23</sup>] We then choose the absorption maxima at  $\sim 10,000$  cm<sup>-1</sup> to be associated with the d-d transition t<sub>1</sub><sup>6</sup>e<sup>1</sup>t<sub>2</sub><sup>0</sup> → t<sub>1</sub><sup>6</sup>e<sup>0</sup>t<sub>2</sub><sup>1</sup> on the basis that the intensity of a transition which involves states of significant d character should be weaker than a metal to ligand, ligand to metal, or ligand to ligand transition. These assignments are consistent with a crystal field splitting energy of  $\sim 10,000$  cm<sup>-1</sup> rather than the value of  $\sim 17,000$  cm<sup>-1</sup> which has been suggested before.<sup>6</sup> This discrepancy must raise serious questions about the ability of some current molecular orbital approaches to predict the crystal field splitting energies even of simple molecules.

**Vibrational Assignment.**—On the lowest energy manifold, vibrational origins can be clearly discerned at 9912 ( $\parallel b$ ) and 10,204 cm<sup>-1</sup> ( $\parallel a$ ). (In the  $\parallel a$  polarization the weak line at  $\sim 9950$  cm<sup>-1</sup> is thought to be the incompletely polarized 9912-cm<sup>-1</sup> absorption.) Both progressions are separated by frequencies of greater than 400 cm<sup>-1</sup>; i.e.:  $a \simeq 450$ ;  $b, \simeq 406$  cm<sup>-1</sup>. Although a fundamental of T<sub>2</sub>( $\nu_4$ ) symmetry occurring at 410 cm<sup>-1</sup> has been reported for CrO<sub>4</sub><sup>3-</sup> in Ca<sub>2</sub>CrO<sub>4</sub>Cl,<sup>12</sup> it seems unlikely that it is this vibration which is associated with both the progressions observed on the  $\sim 10,000$ -cm<sup>-1</sup> manifold. For the 450-cm<sup>-1</sup> frequency, observed in the visible spectrum, to be ascribed to this fundamental would require that the molecule be contracted in the excited state. This in turn could only occur if the transition in question was associated with an electron transfer from a nonbonding or antibonding orbital to a bonding orbital. This is clearly an impossibility no matter what assignment one gives to the 10,000-cm<sup>-1</sup> band. For the progression characterized by a 406-cm<sup>-1</sup> spacing, it is possible that this frequency represents a component of this T<sub>2</sub>( $\nu_4$ ) fundamental. The frequency reduction in the excited state would then perhaps be rather small. A small change in the

(23) See S. Holt and R. Dingle, *Acta Chem. Scand.*, **22**, 1091 (1968), and J. Milstein and S. L. Holt, *Inorg. Chem.*, **8**, 1021 (1969).

excited-state internuclear distance is supported by the intensity pattern of the  $||b$  vibrational progression. This would in turn tend to indicate that what would be the antibonding  $t_2$  orbital in  $T_a$  symmetry is not so strongly antibonding in character in  $D_{2d}$  symmetry.<sup>24</sup> In the  $||a$  polarization it is likely that the exciting mode is a combination of the  $T_2(\nu_4)$  and a lattice vibration. Such a mode is observed at  $\sim 500$   $\text{cm}^{-1}$  in the infrared spectrum of  $\text{Ca}_2\text{CrO}_4\text{Cl}$ .<sup>25</sup>

The analysis of the  $\sim 28,000\text{-cm}^{-1}$  manifold is much more clear-cut and undoubtedly is associated with one of the components of the  $T_2(\nu_3)$  fundamental which occur at 865, 810, and 760  $\text{cm}^{-1}$  in the ground state.

**Electronic Structure.**—Various approximate molecular orbital calculations yield, at best, a reasonable ground-state, "one-electron" energy level diagram. Attempts to assign electronic spectral bands on the basis of these in any case other than  $d^0$  ignores the excited-state electron-electron interactions and have led to a variety of speculations in the  $d^1$  and  $d^2$  cases.<sup>3,6,7,13,18,26</sup> This has, of course, been recognized<sup>4</sup> and some attempt is being made to include a correction for repulsion.<sup>27</sup> One of the more recent and successful efforts has been that of Dahl and Johansen.<sup>10</sup> Their calculations suggest that the correct value of  $\Delta\nu$  for  $\text{MnO}_4^-$  is of the order of 10,000  $\text{cm}^{-1}$  and not 26,000  $\text{cm}^{-1}$  as has been previously supposed.<sup>6</sup> This value agrees closely with our results on  $\text{CrO}_4^{3-}$ ,<sup>14</sup>  $\text{MnO}_4^{3-}$ ,<sup>21</sup> and  $\text{MnO}_4^{2-}$ <sup>28</sup> and prompts us to disregard both our previous tentative assignment made for  $\text{MnO}_4^-$  and assignments made by others for the  $\text{MO}_4^{n-}$  system. Indeed, it is perhaps pertinent here to comment upon the crystal field splitting for various  $\text{MO}_4^{n-}$  ions.

As noted earlier most current interpretations of the absorption spectra of  $\text{MO}_4^{n-}$ , where  $n = 1-3$ , have indicated that  $\Delta$  is a sharply increasing function of formal oxidation state.<sup>6,11</sup> This is clearly seen in the data presented in the center column of Table IV.

Our experimental work, however, belies the validity of the  $\Delta$  values reported for the  $d^1$  systems  $\text{CrO}_4^{3-}$ <sup>14</sup> and  $\text{MnO}_4^{2-}$ ,<sup>28</sup> while the Dahl and Johansen interpretation of the spectra of  $\text{MnO}_4^-$  must be considered to be the correct one.

The newer values of  $\Delta$  which arise from these current efforts are shown in the last column in Table IV along with  $\Delta$  values for a number of other manganese tetrahedral oxyanions.

It will be noted that the values in the right-hand side of Table IV do *not* reflect a large increase in  $\Delta$  with formal oxidation state. Based upon the older values of  $\Delta$  and making the reasonable assumption that changes in effective oxidation state should be reflected by similar variations in  $\Delta$ , we should conclude that the effective

TABLE IV

Complex	Metal formal charge	$\Delta$ , <sup>a</sup> $\text{cm}^{-1}$	$\Delta$ , $\text{cm}^{-1}$
$\text{CrO}_4^{3-}$	5	16,000	10,000 <sup>b</sup>
$\text{CrO}_4^{2-}$	6		$\sim 9,000$ <sup>c</sup>
$\text{MnO}_4^{3-}$	2		4,500 <sup>d</sup>
$\text{MnO}_4^{2-}$	3		7,000 <sup>e</sup>
$\text{MnO}_4^-$	4		10,000 <sup>f</sup>
$\text{MnO}_4^{3-}$	5	11,000	11,000 <sup>g</sup>
$\text{MnO}_4^{2-}$	6	19,000	$\sim 10,000$ <sup>f</sup>
$\text{MnO}_4^-$	7	26,000	$\sim 10,000$ <sup>e</sup>

<sup>a</sup> Reference 6. <sup>b</sup> Reference 14. <sup>c</sup> Reference 10. <sup>d</sup> Estimated from the values given for  $\text{MnO}_6^{10-}$  and  $\text{MnF}_6^{2-}$  by C. K. Jørgensen, "Absorption Spectra and Chemical Bonding in Complexes," Pergamon Press, London, 1962, p 110. <sup>e</sup> Estimated from work of R. Dingle, *Acta Chem. Scand.*, **20**, 33 (1966). <sup>f</sup> Reference 27. <sup>g</sup> References 2, 18, 21.

oxidation state of Mn(VII) in  $\text{MnO}_4^-$  is much larger than that of Mn(VI) in  $\text{MnO}_4^{2-}$  which is in turn much larger than that of Mn(V), etc. This is clearly not true if one considers the newer values of  $\Delta\nu$ . Here, one finds that  $\Delta\nu$  has reached a plateau by the time that the formal charge on the manganese ion has become +5. (This contention derives added support from the reported values of  $\Delta$  for  $\text{CrO}_4^{3-}$  and  $\text{CrO}_4^{2-}$ .) From this we must conclude that the *effective charge upon the manganese ion does not increase beyond that found for Mn(V)*.

**Acknowledgment.**—This work was supported by NSF Grant GP7920.

CONTRIBUTION FROM THE INSTITUTE OF INORGANIC AND ANALYTICAL CHEMISTRY, L. EÖTVÖS UNIVERSITY, BUDAPEST, HUNGARY

### Application of Diffusion Constant Measurement to the Determination of the Rate Constant of Electron-Exchange Reactions

BY I. RUFF AND I. KORÖSI-ÓDOR

Received June 17, 1969

Recently a new method was suggested by I. R. for the determination of the rate constant of very fast electron-exchange reactions,<sup>1</sup> based on Dahms' prediction<sup>2</sup> of the existence of electronic conduction in aqueous solutions. Electronic conduction takes place, when there is a concentration gradient in the solution containing particles of both oxidation states of an oxidation-reduction couple and the gradient of one of them differs from that of the other in every point of the system. For the sake of simplicity, let the system consist of two parts at the time  $t = 0$  which are divided by an imaginary plane at the linear coordinate perpendicular to this plane  $x = 0$ . Let the concentration of the species be  $c_{\text{red}} = 0$  and  $c_{\text{ox}} = c_0$ , if  $x < 0$ , and  $c_{\text{ox}} = 0$

(24) Similar behavior had been reported for  $\text{CoCl}_4^{2-}$ : J. Ferguson, *J. Chem. Phys.*, **39**, 116 (1963).

(25) M. Greenblatt, Ph.D. Thesis, Polytechnic Institute of Brooklyn, June 1967.

(26) H. Basch, A. Viste, and H. B. Gray, *J. Chem. Phys.*, **44**, 10 (1966).

(27) Cf. B. B. Chastain, E. A. Rick, R. L. Pruett, and H. B. Gray, *J. Am. Chem. Soc.*, **90**, 3994 (1968).

(28) C. A. Kosky and S. L. Holt, to be submitted for publication.

(1) I. Ruff, *Electrochim. Acta*, in press.

(2) H. Dahms, *J. Phys. Chem.*, **72**, 362 (1968).